Published OnlineFirst July 27, 2010; DOI: 10.1158/1535-7163.MCT-10-0181

Selective and Potent Raf Inhibitors Paradoxically Stimulate Normal Cell Proliferation and Tumor Growth

Josette Carnahan[1], Pedro J. Beltran[1], Carol Babij[1], Quynh Le[1], Mark J. Rose[2], Steven Vonderfecht[3], Joseph L. Kim[6], Adrian L. Smith[4], Karthik Nagapudi[5], Martin A. Broome[1], Manory Fernando[1], Hue Kha[1], Brian Belmontes[1], Robert Radinsky[1], Richard Kendall[1], and Teresa L. Burgess[1]

Abstract

Raf inhibitors are under clinical investigation, specifically in patients with tumor types harboring frequent activating mutations in B-Raf. Here, we show that cell lines and tumors harboring mutant B-Raf were sensitive to a novel series of Raf inhibitors (e.g., ^{V600E}B-Raf A375, IC_{50} on cells = 2 nmol/L; ED_{50} on tumor xenografts = 1.3 mg/kg). However, in cells and tumors with wild-type B-Raf, exposure to Raf inhibitors resulted in a dose-dependent and sustained activation of mitogen-activated protein kinase signaling. In some of these cell lines, Raf inhibition led to entry into the cell cycle, enhanced proliferation, and significantly stimulated tumor growth *in vivo*. Inhibition with structurally distinct Raf inhibitors or isoform-specific small interfering RNA knockdown of Raf showed that these effects were mediated directly through Raf. Either A-Raf or C-Raf mediated the Raf inhibitor–induced mitogen-activated protein kinase pathway activation in an inhibitor-specific manner. These paradoxical effects of Raf inhibition were seen in malignant and normal cells *in vitro* and *in vivo*. Hyperplasia of normal epithelial cells in the esophagus and the stomach was evident in mice with all efficacious Raf inhibitors (n = 8) tested. An implication of these results is that Raf inhibitors may induce unexpected normal cell and tumor tissue proliferation in patients. *Mol Cancer Ther; 9(8); 2399–410. ©2010 AACR.*

Introduction

The mitogen-activated protein kinase (MAPK) pathway controls cell proliferation and differentiation in normal cells by integrating signals from ligand activation of plasma membrane receptors through RAS, Raf, MAP/extracellular signal-regulated kinase (ERK) kinase (MEK), and then ERK. Once activated, phosphorylated ERK (P-ERK) is translocated to the nucleus where it transcriptionally regulates a variety of gene expression programs controlling normal cell functions (1, 2). The Raf serine-threonine kinase family plays a key role in transmitting and regulating signaling through the MAPK pathway. *B-Raf* and *C-Raf* are essential genes (3–7). Mice with genetic deletion of *A-Raf* are viable, albeit with some tissue-specific defects (6, 8, 9). *B-Raf* seems to be the most potent MAPK pathway activator compared with *C-Raf* and *A-Raf* (6, 10, 11).

Authors' Affiliations: Departments of [1]Hematology & Oncology Research, [2]Pharmacokinetics & Drug Metabolism, [3]Pathology and Comparative Biology Safety Sciences, [4]Medicinal Chemistry, and [5]Pharmaceutics, Amgen, Inc., Thousand Oaks, California; and [6]Department of Molecular Structure, Amgen Inc., Cambridge, Massachusetts

Note: Supplementary material for this article is available at Molecular Cancer Therapeutics Online (http://mct.aacrjournals.org/).

Each author has approved the content of this article.

Corresponding Author: Josette Carnahan, Amgen, Inc., One Amgen Center Drive, Thousand Oaks, CA 91320. Phone: 805-447-4469; Fax: 805-375-8368. E-mail: jcarnaha@amgen.com

doi: 10.1158/1535-7163.MCT-10-0181

Activating mutations in RAS and Raf occur in tumors. Each of these nodes has been explored for therapeutic intervention in oncology with both successes and failures (12–14). Activating mutations in B-Raf are particularly prevalent in melanoma (~60%), thyroid (~35%), and colorectal (~10%) cancers. Among the reported mutations, substitution of valine for glutamic acid at the activation loop residue 600 (V600E) is the most common (~90%) and confers strong kinase activation and transforming properties to B-Raf (15, 16).

The prevalence and dominant effects of B-Raf mutations in tumors led to the identification and development of small-molecule inhibitors targeting Raf (17–21). Preclinical studies showed that cells and tumors harboring ^{V600E}B-Raf were sensitive to Raf inhibition (22). Early-phase clinical studies of selective Raf inhibitors have shown objective clinical responses in some patients with tumors harboring ^{V600E}B-Raf (23, 24).

Here, we report on the *in vitro* and *in vivo* activity of a novel series of highly potent and selective Raf inhibitors (25) across a panel of cell and tumor xenograft models harboring MAPK pathway alterations as well as in normal cells and tissues. We show that MAPK pathway signal modulation correlates with cell, tumor, and normal tissue response to Raf inhibitors. Furthermore, we show that Raf inhibitor–induced stimulation of MAPK signaling can result in increased tumor growth and epithelial cell hyperplasia mediated through A-Raf or C-Raf. An implication of these data is that the treatment of patients with Raf inhibitors may lead to on-mechanism

Published OnlineFirst July 27, 2010; DOI: 10.1158/1535-7163.MCT-10-0181

hyperplasia in normal cells or even stimulation of non-mutant B-Raf tumor growth.

Materials and Methods

Chemical inhibitors

Inhibitors included ZM336372 (26–28), PD-0325901, gefitinib, sorafenib, and UO126.

Biochemical assays

^{V600E}B-Raf (Amgen), truncated ^{WT}B-Raf, $^{Y340D/Y341D}$C-Raf (Millipore), and kinase-dead MEK1-Avitag were used for *in vitro* HTRF assays. Reactions were done in kinase buffer (50 mmol/L Tris/10 mmol/L $MgCl_2$/0.01% bovine serum albumin/0.5 mmol/L DTT) for 1 hour at room temperature. Phosphorylation was detected with LANCE-labeled (Perkin-Elmer) anti–phospho-MEK1 (Cell Signaling) and Streptavidin-APC (Prozyme PJ25S) by reading on a RUBYstar fluorometer (BMG Labtech).

Cellular assays

Cells were from the American Type Culture Collection (unless otherwise noted) and maintained in recommended growth media. Cells were starved by substituting serum with 0.1% bovine serum albumin. M24met cells were acquired from Dr. Barbara Mueller, Torrey Pines Institute for Molecular Studies, San Diego, CA (29). For signaling assays, cells were preincubated with inhibitors for 1 hour unless otherwise noted and harvested for immunoblotting or In Cell Western assays. For viability assays, cells were plated in 96-well plates (Corning) 20 hours before compound addition and assayed after 72 hours using an ATPlite kit (Perkin-Elmer).

Immunoblotting in cell Western assays

Cells were lysed in ice-cold triton lysis buffer [20 mmol/L Tris (pH 7.5)/137 mmol/L NaCl/5 mmol/L EDTA/10% Glycerol/1% Triton X-100] containing protease and phosphatase inhibitors (Sigma). Protein concentration was determined in cleared lysates with a Bio-Rad Dc kit. Antibodies were from Santa Cruz Biotechnology (A-Raf, B-Raf, and C-Raf), Cell Signaling Technology [P-ERK (T202Y204), T-ERK, P-MEK [S217/221], T-EGFR, Cyclin D1, and poly ADP ribose polymerase], and Becton-Dickenson ($p27^{Kip}$), and were confirmed to detect the protein of interest. Antibody detection and In Cell Western assays was done according to LI-COR's protocol. Briefly, fixed cells were probed with rabbit anti–P-ERK (Cell Signaling) and mouse anti-ERK2 (Santa Cruz Biotechnology, Inc.). Anti-rabbit Alexa680 (Molecular Probes) and anti-mouse IRdye800 (Rockland) secondary antibodies were detected by the Odyssey scanner. The ratio of P-ERK to T-ERK was determined, and IC_{50s} were calculated using XL-FIT Version 4.

Flow cytometry

A375 cells on adherent plates (Falcon) and MIA PaCa-2 cells on low-adherent plates (Costar) were treated with Raf inhibitors or the equivalent DMSO concentration (0.1%) for 24 hours. Bromodeoxyuridine (BrdUrd) labeling solution (Invitrogen) was added, and cells were processed according to the manufacturer's protocol. DNA was counterstained with propidium iodide (BD Biosciences). Samples were analyzed on a FACScan flow cytometer (BD Biosciences).

Small interfering RNA transfection

Small interfering RNAs (siRNA) were obtained from Invitrogen (scrambled negative control-MidG/C, B-Raf Stealth duplex#2, C-Raf Stealth duplex#1 siRNA), Qiagen (A-Raf, KRAS), and Dharmacon (A-Raf, KRAS). Cells were transfected with 25 nmol/L of each siRNA using Invitrogen RNAiMAX reagent. Cells were treated 48 hours post-transfection with inhibitors or 0.1% DMSO, and harvested for immunoblotting.

Colony formation assay

MIA PaCa-2 cells were assayed with the CytoSelect soft agar assay kit (Cell Biolabs, Inc.). Briefly, cells were plated in low-adherence plates (Corning) in their normal growth media containing 0.4% soft agar and C-19. A growth media overlay also containing C-19 was added, and cells were grown at 37°C in 5% CO_2 for 7 days.

Animals

Athymic female (4- to 6-wk-old) nude mice (Harlan Laboratories, Inc.) or CD1 *nu/nu* mice (Charles River Laboratories) were housed according to all Association for Assessment and Accreditation of Laboratory Animal Care specifications. Experimental procedures were done in accordance with Institutional Animal Care and Use Committee and United States Department of Agriculture regulations.

Efficacy studies using human xenograft models

The A375 SQ2 cell line was generated by performing two serial *in vivo* passages of A375 cells in CD1 *nu/nu* mice. The resulting tumor cells were reestablished in culture and shown to have identical *in vitro* growth properties. The ^{V600E}B-Raf mutation was verified by genomic sequencing. This procedure optimized tumor take and generated more uniform and reproducible tumor growth. Raf inhibitors were formulated in 2% HPMC, 1% Tween 80 (pH 2.2; vehicle) for oral administration. Five million cells suspended in Matrigel (BD Bioscience) were injected s.c. into athymic nude (MIA PaCa-2) or CD1 *nu/nu* mice (all other cell lines). When tumor volume reached ~200 mm^3, mice were randomly assigned into groups of 10. Oral dosing was done daily or twice daily at the indicated dose for the duration of the experiment. Tumor volume and body weight were measured in a blinded fashion twice per week using calipers and an animal scale. ED_{50} and EC_{50} were calculated from the linear regression of the percent tumor inhibition on the last day of the experiment versus either the dose of inhibitor (ED) used, or the plasma concentration of inhibitor

Published OnlineFirst July 27, 2010; DOI: 10.1158/1535-7163.MCT-10-0181

(EC) obtained, on the last day of the experiment using the GraphPad Prism 5.1 software.

Statistical analysis

Differences in tumor volume and body weight in the treated versus vehicle groups were determined with repeat measurement ANOVA and Scheffe's *post hoc* analysis (StatView software 5.0.1, SAS Institute, Inc.).

Xenograft pharmacodynamic assay

P-ERK and T-ERK were measured in xenograft tumors (n = 2) 2 or 24 hours following the last dose in each efficacy study. Tumors were harvested and snap frozen in liquid nitrogen. Tumor lysates were prepared by homogenization in ice-cold radioimmunoprecipitation assay buffer [50 mmol/L Tris (pH 7.5), 150 mmol/L NaCl, 1% NP40, 0.5% sodium deoxycholate, and 0.1% SDS] containing protease and phosphatase inhibitors (Sigma), assayed using phospho/total ERK1/2 duplex Meso Scale Discovery plates, and analyzed using an Meso Scale Discovery 6000 plate reader.

Analysis of hyperplasia in nontumor-bearing mice

Naïve female CD1 *nu/nu* mice (4- to 6-wk-old) were treated twice daily orally with inhibitors or vehicle alone for 6 days (total of 12 doses). On day 7, 2 hours after the final dose, mice were injected with BrdUrd reagent and sacrificed 2 hours later. The esophagus and nonglandular stomachs were collected, processed, embedded in paraffin, sectioned, and stained with H&E, and for BrdUrd incorporation, by an immunohistochemical method to detect BrdUrd incorporation. All sections were examined by routine light microscopy and without knowledge of the treatment group.

Immunohistochemical detection of BrdUrd label

Deparaffinized tissue sections were digested with 0.1% protease (Sigma) and treated with 2N hydrochloric acid. Following blockage with CAS BLOCK (Zymed Laboratories), sections were sequentially incubated with rat anti-BrdUrd antibody (Accurate), biotinylated rabbit anti-rat IgG (Vector Laboratories), peroxidase blocking solution (DAKO Corp.), and Vectastain Elite ABC kit (Vector Laboratories). Reaction sites were visualized with a 3,3′-diaminobenzidine + Substrate-Chromagen System (DAKO Corp.).

Results

A novel series of kinase inhibitors showed potent biochemical activity

A description of the activity, selectivity, and syntheses of the full series of Raf inhibitors used here is presented elsewhere (25). The chemical structures and biochemical potencies of selected inhibitors are shown in Supplementary Fig. S1 and Table S1. Compound 1 (C-1) showed the greatest potency of the series (^{WT}B-Raf Ki = 1 nmol/L, ^{V600E}B-Raf Ki = 1 nmol/L, and C-Raf Ki = 0.3 nmol/L). Compound 19 (C-19), although less potent, (^{WT}B-Raf Ki = 21 nmol/L, ^{V600E}B-Raf Ki = 42 nmol/L, and C-Raf Ki = 21 nmol/L) proved to be a useful tool compound *in vitro*.

Inhibition of MAPK pathway signaling by Raf inhibitors correlated with suppression of cell viability and delay of cell cycle progression in $^{V600E/D}$B-Raf cells

Both C-1 and C-19 showed robust inhibition of P-ERK levels in ^{V600E}B-Raf A375 cells with IC_{50}s of 2 and 28 nmol/L, respectively (Supplementary Table S1). Dose-dependent downregulation of P-ERK by C-19 was confirmed by immunoblot (Fig. 1A). Additionally, C-1 and C-19 each caused a corresponding dose-dependent inhibition of cell viability (Table 1; Fig. 1C).

Cell cycle analysis of A375 cells showed that C-19 induced a dose-dependent decrease in the percentage of cells in S phase, a slight increase in the percentage of cells in G_1, and a clear increase in the percentage of cells in the sub-G_1 peak (dead cells; Fig. 1B). C-1 and C-19 caused cell cycle arrest (decreased cyclin D1 and increased $p27^{Kip}$) and induced apoptosis (increased poly ADP ribose polymerase cleavage) in A375 cells (Supplementary Fig. S2, left). Raf inhibition by C-1 also inhibited MAPK pathway signaling and cell viability in A375 and four other cell lines harboring ^{V600E}-B-Raf or ^{V600D}-B-Raf mutations (Table 1).

Cell lines with either non-Raf MAPK pathway mutations (e.g., NRAS or KRAS; n = 5) or without pathway mutations (n = 3) generally had higher IC_{50}s *in vitro* compared with cell lines with B-Raf mutations (Table 1). Similar results were obtained with all Raf inhibitors tested (n = 8), including compounds with distinct chemical structures (data not shown).

Raf inhibition resulted in tumor growth inhibition in some xenograft models

To investigate the efficacy of Raf inhibitors *in vivo*, established tumor xenografts from seven different cell lines harboring ^{V600E}B-Raf, NRAS, or KRAS pathway mutations were treated with a dose range of C-1 (Supplementary Table S2; Fig. 2A–D), chosen based on its optimal potency and favorable pharmacokinetic properties (25). Tumor volume measurements over time are shown (Supplementary Table S2; Fig. 2A–D, left). All dose regimens were well tolerated with no significant treatment-related weight loss observed (Supplementary Fig. S3). A375 SQ2 xenografts were the most sensitive to Raf inhibition: C-1 induced significant tumor growth inhibition (TGI) at 1 mg/kg (91% TGI) and 2 mg/kg (100% TGI), and significant tumor regression (85%) at 5 mg/kg daily (Fig. 2A). Linear regression analysis between TGI and serum concentrations of C-1 on the last day of the experiment yielded an ED_{50} of 1.3 mg/kg ($AUC_{0\text{-}24h}$ = 2.7 μg.h/L) for A375 SQ2 tumor xenografts. C-1 showed efficacy in two other mutant B-Raf tumor models, with similar ED_{50} value to A375 SQ2 (Supplementary Table S2).

Published OnlineFirst July 27, 2010; DOI: 10.1158/1535-7163.MCT-10-0181

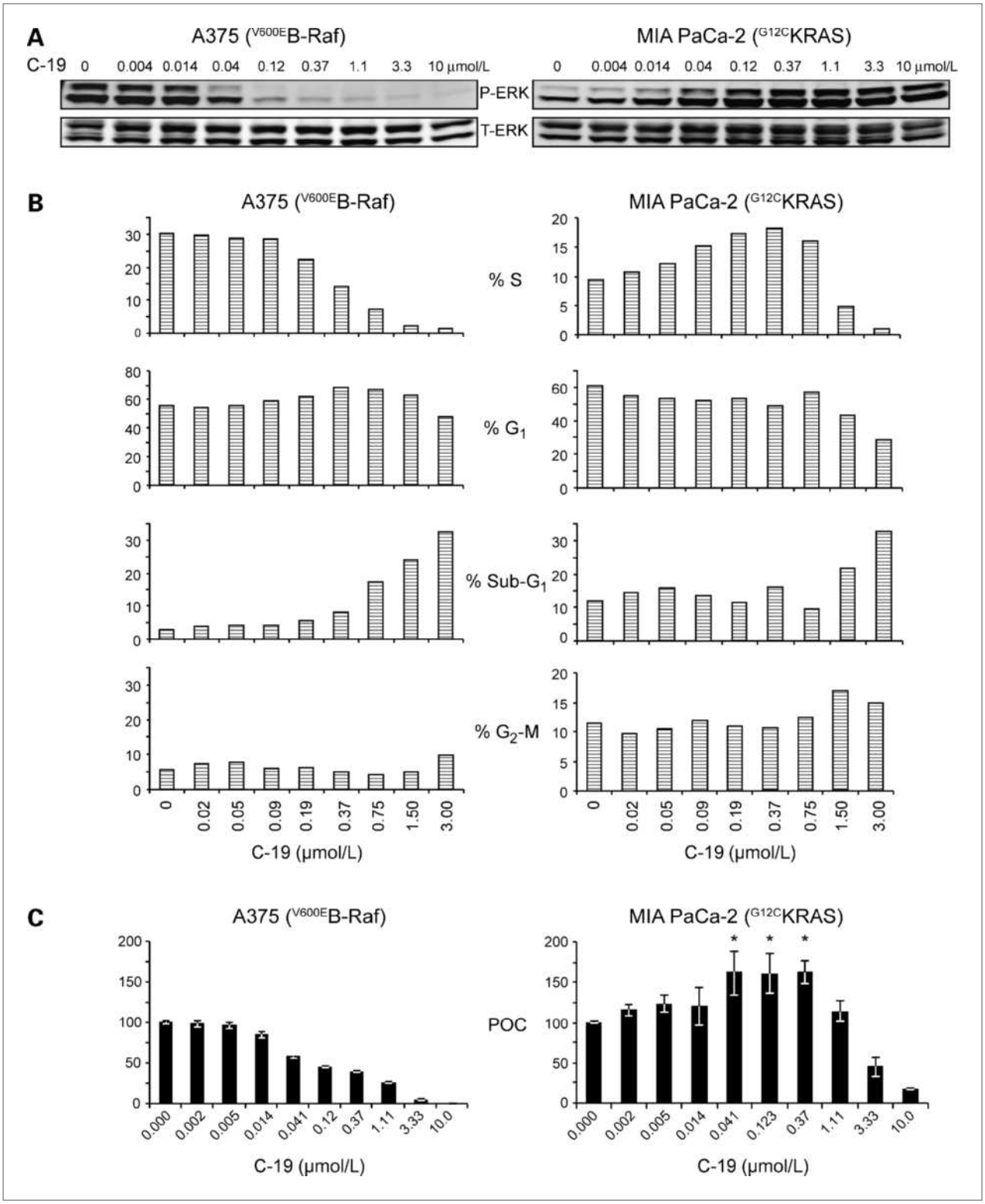

Figure 1. The effect of Raf inhibition on MAPK signaling, cell cycle, and cell viability in cell lines with B-Raf or KRAS mutations. A, levels of P-ERK in A375 (^{V600E}B-Raf) and MIA PaCa-2 (^{G12C}KRAS) cells determined by immunoblotting. T-ERK was the loading control. B, cells were treated with C-19 for 24 h and pulsed with BrdUrd for 1 h before harvest. The percentages of cells in S (BrdUrd positive), G1, sub-G_1, and G_2-M phases were determined by flow cytometry (representative data from three experiments). C, cells were treated with C-19 for 3 d, and viability was measured using an ATPlite assay. Columns, mean; bars, SD. *, $P < 0.01$ one-way ANOVA/Dunnett's Multiple Comparison test (representative data from four experiments).

Published OnlineFirst July 27, 2010; DOI: 10.1158/1535-7163.MCT-10-0181

Table 1. The effect of Raf inhibitor C-1 on signaling and viability in cell lines with WT and mutated MAPK pathway genes

Cells	Mutation status		Cell assay IC_{50} (μmol/L)	
	B-Raf	RAS	P-ERK	Cell viability
A375	V600E	WT	0.002	0.31
WM-266-4	V600D	WT	0.003	0.04
SK-MEL-28	V600E	WT	0.003	0.11
Colo-205	V600E	WT	0.014	0.15
Sk-Mel2	WT	^{Q61R}NRAS	0.26	0.29
M24met	WT	^{Q61R}NRAS	0.85	1.80
A549	WT	^{G12S}KRAS	4.96	2.84
HCT-116	WT	^{G13D}KRAS	0.45	0.72
MIA PaCa-2	WT	^{G12C}KRAS	5.70	2.18
A431	WT	WT	ND	2.44
HeLa + EGF	WT	WT	4.20	1.70
NHF + bFGF	WT	WT	2.70	1.64

Abbreviations: NHF, normal human fibroblast; bFGF, basic fibroblast growth factor; ND, not done.

The mutant ^{Q61R}NRAS melanoma model M24met and the mutant ^{G13D}KRAS colon carcinoma model HCT-116 (30) were less sensitive to C-1 than the A375 SQ2; higher doses of C-1 were required to achieve approximately 90% and 40% TGI in M24met and HCT-116, respectively (Fig. 2B and C).

Raf inhibitor treatment resulted in an unexpected stimulation of tumor growth in ^{G12C}KRAS MIA PaCa-2 tumors

In contrast to the TGI observed in the NRAS and KRAS mutant tumor models, C-1 was not efficacious in the mutant ^{G12S}KRAS lung adenocarcinoma tumor model A549 (Supplementary Table S2). Most strikingly, treatment with C-1 led to statistically significant tumor growth stimulation (TGS) in the mutant ^{G12C}KRAS pancreatic carcinoma tumor model MIA PaCa-2 (Fig. 2D). TGS was replicated twice with C-1, and a trend toward TGS was observed (data not shown) with the less potent Raf inhibitor, C-15 (Supplementary Fig. S1, Supplementary Table S1).

Raf inhibitor–induced changes in MAPK pathway signaling correlated with tumor growth modulation in all xenograft models tested

Because TGS by Raf inhibition was unexpected, we investigated the MAPK pathway modulation in the tumor efficacy studies detailed above. Inhibition of MAPK pathway activation in A375 SQ2 tumors following 2 weeks of repeated dosing closely mirrored efficacy, with significant TGI occurring when P-ERK levels fell below 30% of control (Fig. 2A, right). A similar correlation between MAPK pathway modulation and efficacy was observed in two other mutant B-Raf tumor models, Colo-205 and WM-266-4 (Supplementary Table S2). Daily dosing of C-1 resulted in the downregulation of P-ERK in M24met (^{Q61R}NRAS) and HCT-116 (^{G13D}KRAS) tumors that correlated with TGI (Fig. 2B and C, right).

In contrast, the unexpected Raf inhibitor–induced TGS of MIA PaCa-2 (^{G12C}KRAS) xenograft tumors was accompanied by a sharp and statistically significant increase in P-ERK/T-ERK ratios 24 hours postdosing (Fig. 2D, right). Analysis of P-ERK/T-ERK at the 24-hours time point in the HCT-116 (^{G13D}KRAS) model showed no stimulation. B-Raf mutant models were examined up to 12 hours postdosing and showed no stimulation of P-ERK/T-ERK signaling (Supplementary Fig. S4).

Raf inhibition differentially affected MAPK signaling, cell cycle, and viability in different cell backgrounds

To investigate the conundrum that Raf inhibition could lead to MAPK pathway inhibition or stimulation, and result in TGI or TGS, we investigated the effects of Raf inhibition on signaling, cell viability, and cell cycle progression in MIA PaCa-2 (^{G12C}KRAS) cells (Fig. 1A–C, right) similar to that performed on ^{V600E}B-Raf A375 melanoma cells (Fig. 1A–C, left). In MIA PaCa-2 cells (right) treated with C-19, P-ERK levels followed a bell-shaped dose response (Fig. 1A), and high P-ERK levels were strongly associated with entry into the cell cycle (Fig. 1B), cell viability (Fig. 1C), and soft agar colony formation (Supplementary Fig. S5A). In contrast to Raf inhibition in A375 cells, changes in Cyclin D1, $p27^{KiP}$, and poly ADP ribose polymerase cleavage were not observed (Supplementary Fig. S2, right). Similar results were observed with other potent Raf inhibitors in MIA PaCa-2 cells ($n = 7$; data not shown). Treatment with sorafenib resulted in a moderate MAPK activation, consistent with its reduced cell potency on Raf (Supplementary Fig. S5B).

Stimulation of the MAPK pathway by Raf inhibition was increased and prolonged relative to growth factor stimulation and was sensitive to pathway inhibitors, both upstream (epidermal growth factor receptor) and downstream (MEK) of Raf

We compared MAPK pathway activation by Raf inhibitors versus physiologic pathway activation by ligand. Elevation of P-ERK in epidermal growth factor (EGF)– or C-19–treated cells began within 10 minutes, suggesting a direct effect of the inhibitor on Raf (Fig. 3A, top). As expected, P-ERK levels rapidly returned to the basal state in EGF-treated cells (reviewed in ref. 2). In contrast, C-19 treatment increased both the extent and duration of P-ERK activation (Fig. 3A, bottom). We investigated if ligand stimulation could be enhanced by pretreatment with C-19. P-MEK and P-ERK were further elevated by fetal bovine serum or EGF in MIA PaCa-2 cells when pretreated for 1 hour with C-19 compared with cells treated with ligand alone (Fig. 3B, bottom, lane 3 versus 4, and 5 versus 6). A similar enhancement of ligand stimulation by Raf inhibitors was observed in other WT

Published OnlineFirst July 27, 2010; DOI: 10.1158/1535-7163.MCT-10-0181

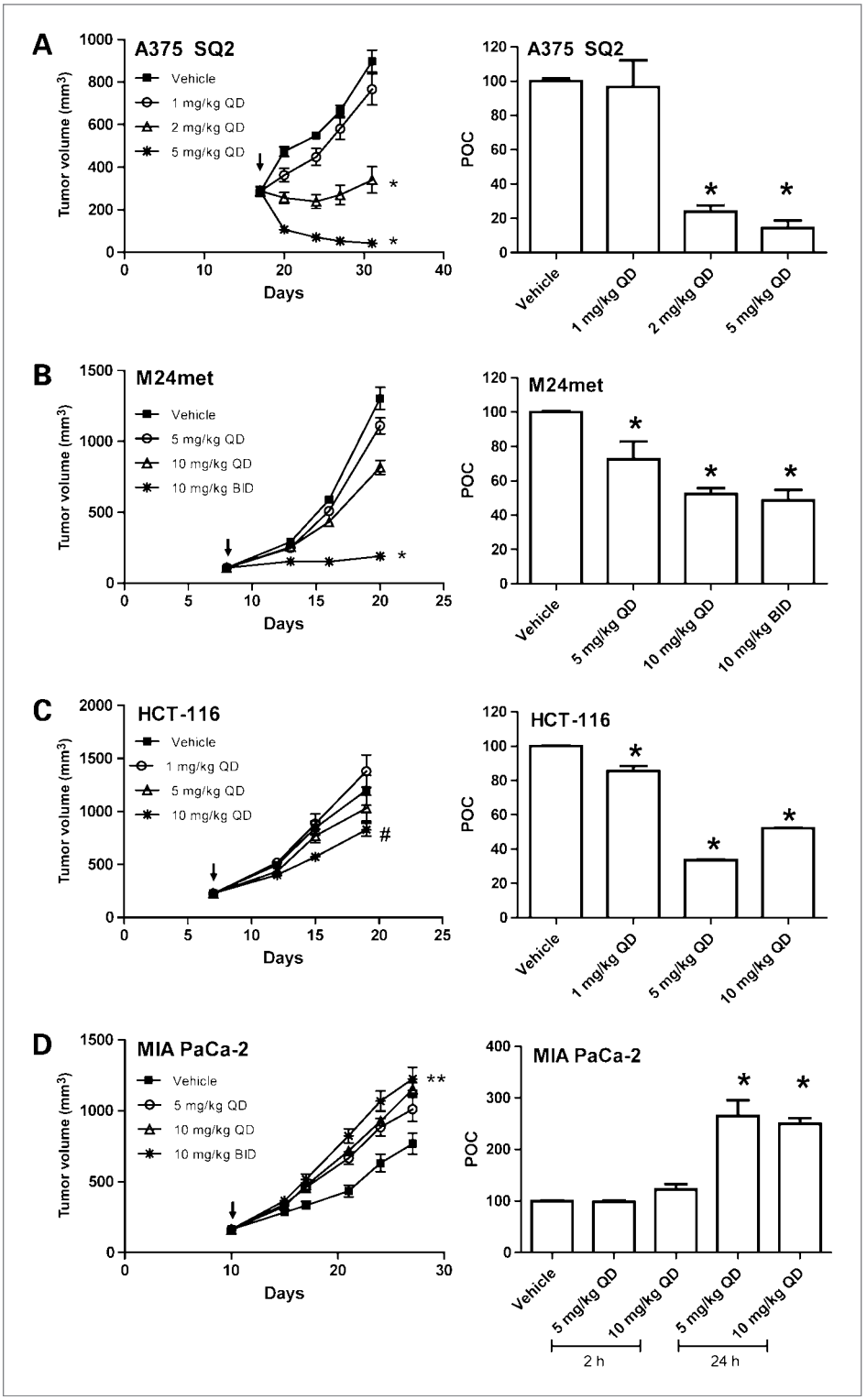

Figure 2. The effect of Raf inhibition on tumor growth and MAPK signaling in xenograft tumor models with pathway mutations in B-Raf (A375 SQ2), NRAS (M24met), or KRAS (HCT-116 and MIA PaCa-2). A to D, left, CD1 *nu/nu* (A–C) and athymic (D) mice were injected with tumor cells and randomized into groups of 10 based on tumor volume (approximately 200–300 mm^3). Treatment with C-1 began on the day indicated by the arrow and continued daily (QD) or twice daily (BID) for the duration of the experiment. Tumor volumes (measured twice per week) are shown as mean ± SEM. *, $P < 0.0001$; **, $P = 0.0025$; and #, $P = 0.089$ determined with RMANOVA and *post hoc* Scheffe test. A–D, right, two xenograft tumors/group were collected 2 h (or as noted otherwise) after the last dose and processed for P-ERK/T-ERK analysis in triplicate using the Meso Scale Discovery assay. Data are expressed as percent of control (POC), and values are shown as mean + SEM. *, $P < 0.006$ determined with ANOVA with *post hoc* Bonferroni test. Experiments were repeated at least twice.

(wild-type) B-Raf cell lines (data not shown). In contrast, C-19 reduced the EGF-induced P-MEK and P-ERK (lane 1 versus 5) stimulation of A375 (^{V600E}B-Raf) cells (Fig. 3B, top, lane 5 versus 6).

Next, we investigated the role of signaling elements upstream (EGF receptor) and downstream (MEK) of Raf in C-19–treated cells. The A431 cell line has a genetically WT MAPK pathway with a low basal level of

Published OnlineFirst July 27, 2010; DOI: 10.1158/1535-7163.MCT-10-0181

P-ERK, although it harbors overexpressed and constitutively activated EGF receptor (Fig. 3C; ref. 31). We tested C-19 in these cells with and without the tyrosine kinase inhibitor gefitinib (32) to block EGF receptor activation.

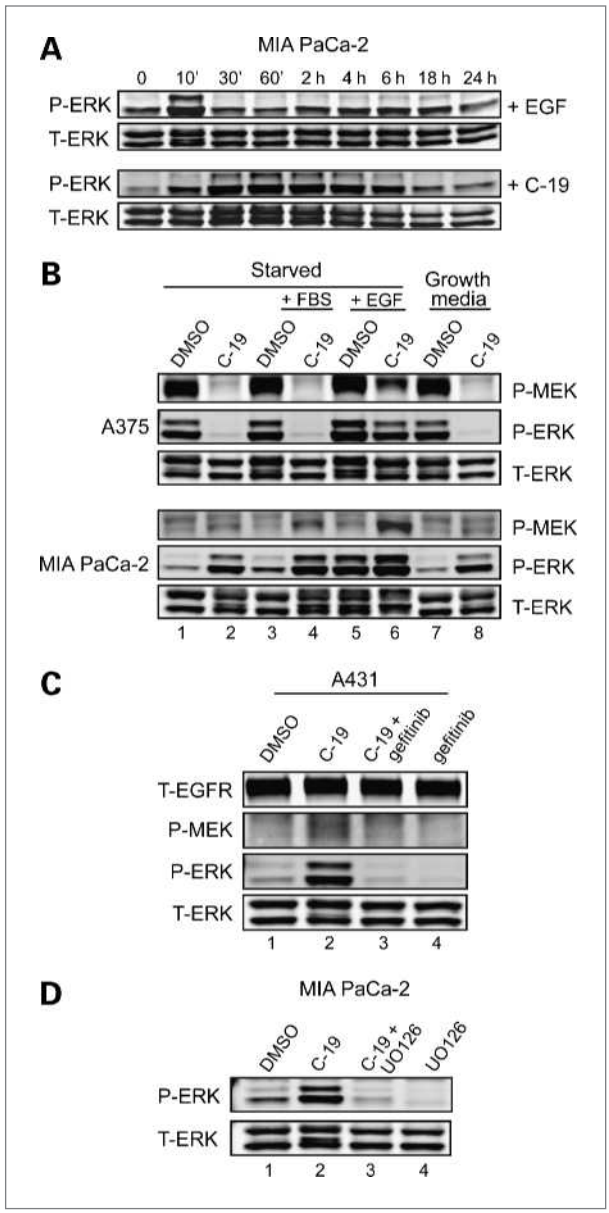

Figure 3. MAPK signaling in cells treated with Raf inhibitors, with and without growth factor stimulation or pathway inhibition. Cells were treated as described, and the MAPK pathway activation status was assayed by immunoblotting. A, MIA PaCa-2 (^{G12C}KRAS) cells were treated with 1 μmol/L C-19 or 20 ng/mL EGF for the noted time points. B, A375 (^{V600E}B-Raf) or MIA PaCa-2 cells (starved overnight or left in growth media) were treated with 0.1% DMSO or 1 μmol/L C-19 for 1 h followed by 20 ng/mL FBS or EGF for 10 min. C, A431 cells were treated with 0.1% DMSO, 1 μmol/L C-19, 1 μmol/L gefitinib, or 1 μmol/L C-19 plus 1 μmol/L gefitinib for 1 h. D, MIA PaCa-2 cells were treated with 0.1% DMSO, 1 μmol/L C-19, 1 μmol/L UO126, or 1 μmol/L C-19 plus 1 μmol/L UO126 for 1 h.

Gefitinib treatment alone decreased the low basal P-ERK (Fig. 3C, lane 1 versus 4), whereas treatment with C-19 resulted in a significant increase in P-MEK and P-ERK (Fig. 3C, lane 1 versus 2). Gefitinib treatment prevented the Raf inhibitor–mediated MEK and ERK phosphorylation (Fig. 3C, lane 2 versus 3).

To test if signaling downstream of Raf was involved in Raf inhibitor–induced P-ERK elevation, we tested the selective MEK inhibitor UO126 (33) in combination with C-19 in MIA PaCa-2 cells. C-19 alone induced P-ERK elevation (Fig. 3D, lane 1 versus 2), whereas UO126 completely blocked C-19–induced ERK activation (Fig. 3D, lane 2 versus 3). Inhibition of MEK in nontreated cells completely inhibited basal P-ERK (Fig. 3D, lane 1 versus 4).

Modulation of the MAPK pathway by Raf inhibitors is mediated by activated RAS and specific Raf isoforms

To investigate the mechanism of Raf inhibitor–induced activation of the MAPK pathway, we knocked down the expression of KRAS and each Raf isoform. When KRAS expression was knocked down in MIA PaCa-2 cells using two independent siRNA triggers, basal P-ERK levels were reduced, and the C-19–induced-P-ERK increase was attenuated (Fig. 4A). No change in the expression of the nontargeted Raf isoforms or MEK was observed (data not shown).

The role of the different Raf isoforms in MAPK pathway activation by C-19 was examined. Transfection of MIA PaCa-2 with Raf isoform–selective siRNAs resulted in ~80% reduction of B-Raf or C-Raf protein expression and ~65% reduction of A-Raf protein (Fig. 4B, lanes 1–3 versus 4–18). Raf isoform knockdown in MIA PaCa-2 cells (^{G12C}KRAS) with individual siRNAs showed that C-Raf significantly regulates basal P-ERK levels in DMSO-treated control cells (Fig. 4B, lane 1 versus 10), whereas knockdown of A-Raf or B-Raf had little effect on basal P-ERK levels (lane 1 versus 4 and 7).

In MIA PaCa-2 cells, C-19–induced increases in P-ERK were observed when B-Raf and C-Raf were knocked down alone or in combination (Fig. 4B, lanes 1 and 2 versus lanes 7 and 8, 10 and 11, 13 and 14). In contrast, A-Raf knockdown blocked the C-19–induced increase in P-ERK in MIA PaCa-2 (Fig. 4B, lane 1 and 2 versus 4 and 5) and was seen with multiple independent siRNA triggers (Supplementary Fig. S6). A similar dependence on A-Raf was also observed for all active structural analogues of C-19 tested ($n = 8$). C-19 modulation of P-ERK was also A-Raf dependent in the ^{G12S}KRAS cell line A549 (Supplementary Fig. S7A). Control experiments confirmed that constitutive MAPK pathway activation in the A375 cell line was dependent on ^{V600E}B-Raf. P-ERK was downmodulated by either B-Raf knockdown or C-19 treatment (Supplementary Fig. S7B). The constitutively activated MAPK pathway in A375 was inhibited with all active Raf inhibitors tested ($n = 12$), including compounds with distinct chemical structures (data not shown).

Published OnlineFirst July 27, 2010; DOI: 10.1158/1535-7163.MCT-10-0181

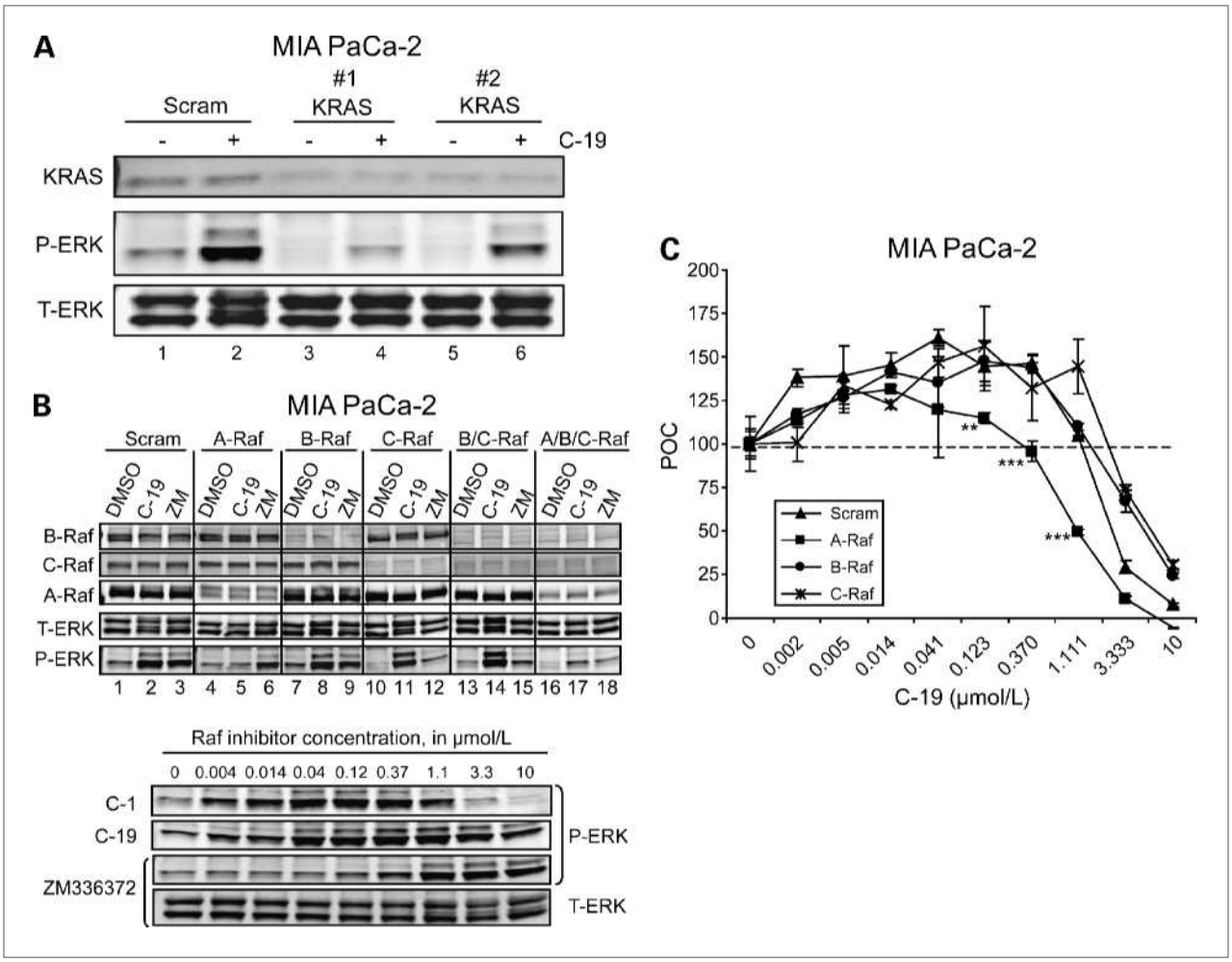

Figure 4. MAPK signaling and cell viability in MIA PaCa-2 (^{G12C}KRAS) and A375 (^{V600E}B-Raf) cells treated with Raf inhibitors, with and without siRNA knockdown of KRAS, A-Raf, B-Raf, or C-Raf. A, MIA PaCa-2 cells were transfected with control, scrambled siRNA (scram), or two independent siRNA to KRAS. Forty-eight hours posttransfection, DMSO (–) or 1 µmol/L C-19 (+) was added to cell culture for 1 h. Cells were assayed by immunoblotting. B, top, MIA PaCa-2 cells were transfected with either control, scrambled siRNA, or siRNA to A-Raf, B-Raf, or C-Raf, or in combination. Forty-eight hours posttransfection, 0.1% DMSO, 1 µmol/L C-19, or 1 µmol/L ZM336372 (ZM) was added to cells for 1 h. Bottom, MIA PaCa-2 cells were treated with increasing concentrations of C-1, C-19, or ZM336372 for 1 h. Cells were assayed by immunoblotting. Total ERK (T-ERK) was used as a loading control on immunoblots. C, MIA PaCa-2 cells were transfected with Raf-isoform selective or control scrambled siRNA, plated on low-adherence plates, and C-19 was added 24 h later. Three days posttreatment, cell viability was measured using an ATPlite assay. ***, $P < 0.001$; **$P < 0.01$ two-way ANOVA/Bonferroni test.

Consistent with the mechanisms described above, siRNA knockdown of A-Raf but not B-Raf or C-Raf significantly reduced the C-19–induced increased viability of MIA PaCa-2 cells (Fig. 4C) and resulted in the lowering the IC_{50} from 1.62 to 0.96 µmol/L.

Different Raf isoforms mediated MAPK pathway activation in a compound-specific manner

A select subset of the assays described above was extended with a panel of known Raf inhibitors. Activation of the MAPK pathway was previously reported for structurally different Raf inhibitors including ZM336372 (Supplementary Fig. S1; refs. 26–28, 34). MIA PaCa-2 cells treated with ZM336372 also showed a dose-dependent increase in P-ERK. Consistent with its lower potency in enzyme and cell assays (Supplementary Table S1), MAPK pathway activation by ZM336372 occurred at higher concentrations compared with either C-19 or C-1 (Fig. 4B, bottom). Unlike C-19 and its structural analogues, only knockdown of C-Raf expression attenuated the increase in P-ERK in cells treated with ZM336372 (Fig. 4B, top, lanes 3, 6, and 9 versus 12, 15, and 18). Twelve selective Raf inhibitors (representing four different structural classes) induced MAPK pathway signaling in MIA PaCa-2 cells and all other tested RAS mutant cell lines ($n = 5$) including A549 (Supplementary Fig. S7A). In each case, there was a clear dependence on only A-Raf or C-Raf based on siRNA knockdown (data not shown). In

Published OnlineFirst July 27, 2010; DOI: 10.1158/1535-7163.MCT-10-0181

addition, the multikinase inhibitor sorafenib induced MAPK activation in MIA PaCa-2 cells, although to a lower extent (Supplementary Fig. S5B) in a C-Raf–dependent manner (data not shown).

Systemic administration of Raf inhibitors resulted in increased proliferation and hyperplasia in normal tissues of mice

After 7 days of treatment with C-19, hyperplasia and hyperkeratosis of the stratified squamous epithelium in the esophagus (data not shown) and nonglandular stomach were observed (Fig. 5, left), and BrdUrd incorporation into cells in the basal layer of the target epithelium was markedly increased (Fig. 5, right). These changes were observed with each potent Raf inhibitor tested (n = 8), including those from two different chemical classes, which were independent of the route of administration (oral or intraperitoneal), and were detected as early as 2 days posttreatment (data not shown).

In vitro, we found that MAPK pathway activation by C-19 (Fig. 3D) was dependent on MEK. To determine if hyperplasia in normal tissue was also dependent on

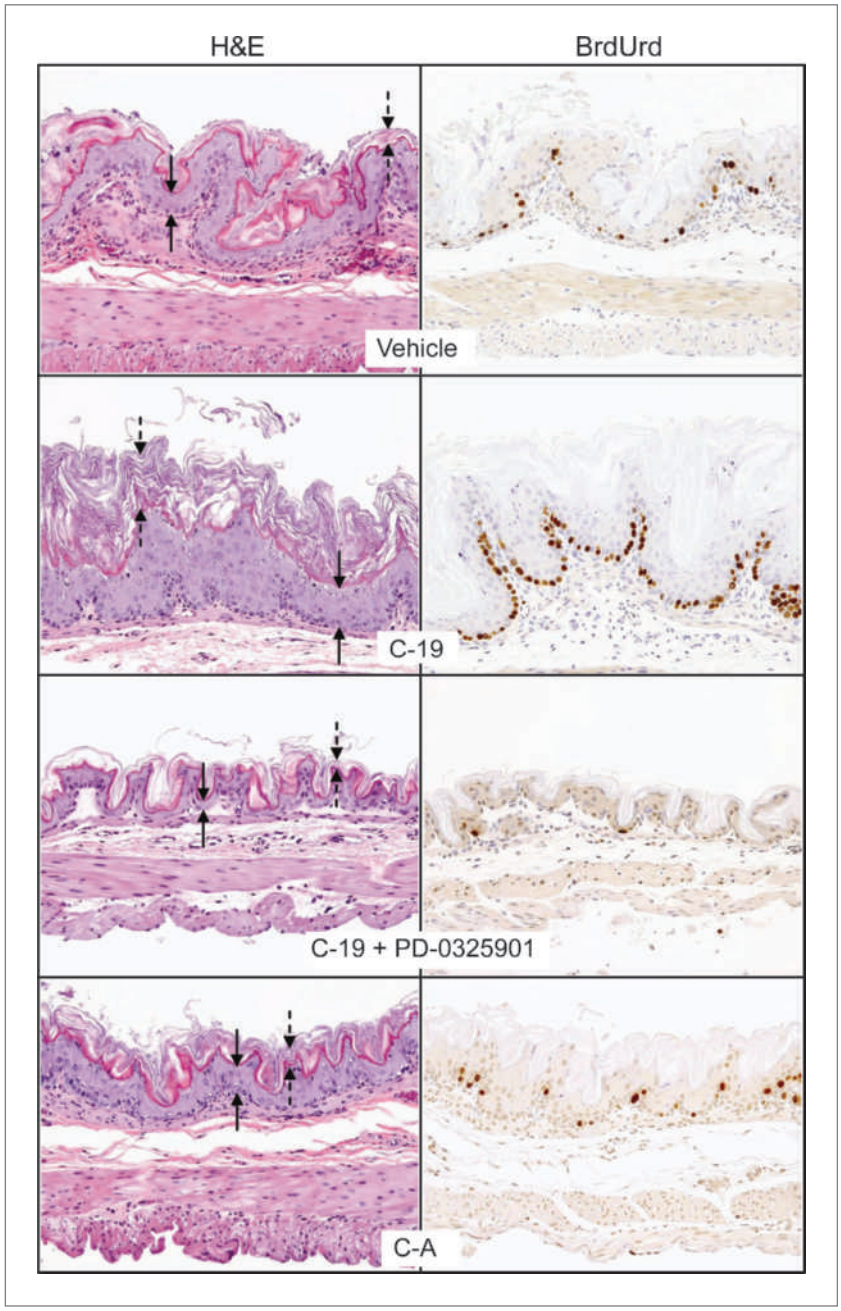

Figure 5. Histopathology and proliferation analysis of epithelial tissues from Raf inhibitor–treated mice. Sections of nonglandular stomach from mice treated orally for 7 d with vehicle (top), 100 mg/kg C-19 twice daily (second row panels), 100 mg/kg C-19 twice daily plus 3 mg/kg PD-0325901 once daily (third row panels), or 35 mg/kg C-A twice daily (bottom) were stained with H&E (left) or for incorporation of BrdUrd (right). Epithelial cells layers (solid arrows) and keratin layers (dashed arrows) are shown. Magnification is ×200.

Published OnlineFirst July 27, 2010; DOI: 10.1158/1535-7163.MCT-10-0181

MEK, we administered C-19 in combination with the MEK inhibitor PD-0325901. There was no resulting hyperplasia or increased BrdUrd incorporation in the epithelium of C-19 cotreated with PD-0325901 mice (Fig. 5). A similar blockade of hyperplasia was observed with animals treated with C-1 in combination with the MEK inhibitor (data not shown). Treatment with PD-0325901 alone did not result in any noticeable histologic changes (data not shown). Finally, although C-A is structurally related to C-19 (Supplementary Fig. S1), it was significantly less active against Raf (Supplementary Table S1). When animals were dosed with C-A, there was no evidence of hyperplasia or increased BrdUrd incorporation (Fig. 5, compare vehicle to C-A), although the plasma concentration of C-A (6 h postdosing) was 1,962 ng/mL, similar to the level of C-19 (1,600 ng/mL) that induces hyperplasia.

Discussion

Here, we describe the biological activity of a novel series of potent Raf inhibitors (25). As expected and previously reported (18, 20, 21), cell lines and tumors harboring mutant B-Raf were sensitive to Raf inhibition. In contrast, cell lines with a WT MAPK pathway or with non-Raf MAPK pathway mutations (e.g., activated KRAS) showed dose-dependent activation of MAPK signaling. In some of these cell lines, Raf inhibition led to increased and sustained MAPK pathway activation, entry into the cell cycle, enhanced proliferation, and significantly stimulated tumor growth *in vivo*. Pharmacologic inhibition of Raf with structurally distinct Raf inhibitors or knockdown of Raf with isoform-specific siRNA showed that these effects were mediated directly through Raf kinases. Either A-Raf or C-Raf mediated the Raf-inhibitor–induced MAPK pathway activation in a compound-specific manner. These paradoxical effects of Raf inhibition were seen in malignant and normal cells, *in vitro* and *in vivo*. Hyperplasia of normal epithelial cells was evident in mice with all efficacious Raf inhibitors tested ($n = 8$), including Raf inhibitors from two different chemical classes. These results point to mechanisms whereby modulation of Rafs by inhibitor binding leads to activation of the MAPK pathway downstream of Raf that is manifested as cell proliferation/hyperplasia in normal tissues. A clear implication of these results is that Raf inhibitors may induce unexpected normal cell or tumor tissue proliferation in patients.

MAPK signaling in normal cells is controlled by positive and negative feedback loops that modulate/attenuate the extent and duration of MAPK pathway activation signaling. Negative feedback loops seem to contribute to pathway inactivation and normal control of cell growth and differentiation (35). Although MAPK pathway activation has been observed with other Raf inhibitors in tumor cell lines (18, 20, 34), a direct correlation between pathway modulation (stimulation or inhibition) and proliferation, cell cycle entry, and tumor growth has not been established. We hypothesize that normal negative feedback control on the MAPK pathway at the level of A-Raf and/or C-Raf is inactivated or prevented by Raf inhibition leading to enhanced and extended signaling. In addition to MAPK pathway activation, it has been reported that Raf inhibitors stabilize and/or favor formation of B-Raf and C-Raf heterodimers (36–38) and increased Raf basal kinase activity. We have observed similar effects with our inhibitors, i.e., C-Raf and A-Raf isolated from cells treated with inhibitors exhibit higher basal kinase activity, and Raf isoform heterodimerization results from treatment only in the WT but not mutant B-Raf cell lines (data not shown).

Either at high concentrations of Raf inhibitors or at later time points, signaling through the MAPK pathway was blocked, and proliferation could be inhibited *in vitro*. However, in certain cells, the sustained pathway activation triggered entry into the cell cycle, enhanced proliferation *in vitro*, and significantly stimulated tumor growth *in vivo*. Hoeflich et al. (21) similarly reported that Raf inhibition with GDC-0879 led to a modest increase in the tumor doubling rate in two of six primary non–small cell lung cancer tumor isolates, with an apparent correlation with B-Raf and RAS mutational status and P-MEK/P-ERK modulation.

A major finding in our studies is that all efficacious Raf inhibitors tested, including those from different chemical classes, caused rapid onset of hyperplasia in mouse epithelial cells of the esophagus and stomach. Evidence of Raf inhibitor–related hyperplasia was also observed in multiple epithelial tissues (stratified squamous epithelia of esophagus, nonglandular stomach, skin, and footpad; transitional epithelia of urinary bladder, renal pelvis and ureter; and bile ducts) as well as in nonepithelial cells (heart and sciatic nerve) of rats and canines (Amgen, data on file; ref. 39). In addition, it was recently reported that treatment with a structurally distinct Raf inhibitor (GDC-0879) led to murine skin acanthosis and hyperkeratosis (21, 38). Taken together, these data suggest that pharmacologic inhibition of Raf may result in homeostatic changes in selected epithelia, and is consistent with clinical observations of frequent hyperkeratosis (40) and a case of skin hyperplasia (41) in patients treated with the multikinase Raf inhibitor sorafenib.

Tumor progression is thought to occur by a multistep transition of normal cells through a hyperplastic, then dysplastic, and finally neoplastic state that is often driven by a series of genetic and/or epigenetic changes. The appearance of squamous cell carcinoma in patients treated with the multikinase Raf inhibitor sorafenib (42) suggests that Raf inhibition could contribute not only to normal and premalignant cell growth but also to tumor progression. Moreover, the treatment-related occurrence of squamous cell carcinoma with the more potent and selective Raf inhibitor PLX4032 was noted in 23% of the patients in phase 1 clinical trials (23). PLX4032 can also cause pathway activation in cells with a WT MAPK pathway (43). Recent reports (37, 38) and our own

Published OnlineFirst July 27, 2010; DOI: 10.1158/1535-7163.MCT-10-0181

unpublished data[7] have shown that Raf inhibitors can profoundly alter MAPK homeostasis in nonmutant B-Raf cells. Thus, Raf catalytic activity may be regulated through conformational changes that result from inhibitor occupation of the kinase ATP binding site. Oligomerization of Raf isoforms, normally a transient event triggered by physiologic stimulation, might be stabilized by inhibitors leading to an aberrant MAPK activation. As shown in this report, this series of events can lead to cell proliferation.

The results presented here correlating MAPK pathway activation by Raf inhibitors with hyperplasia in internal organs may make it difficult to separate the desired clinical efficacy of Raf inhibitors on mutant B-Raf tumors from uncontrolled stimulation of cell growth in normal tissues. A full understanding of the molecular mechanisms controlling the delicate balance between cell proliferation and cell death, and underlying these undesirable consequences of Raf inhibition may elucidate novel clinical strategies for patients with Raf/RAS pathway alterations.

[7] Unpublished data.

Disclosure of Potential Conflicts of Interest

All the authors are current employees of Amgen Inc. and own stock in the company.

Acknowledgments

We thank our colleagues from the B-Raf team: Raju Subramanian, Cecile Savarin, Shawn Walker, Stefan Ruepp, Cindy Afshari, John Wisler, Harvey Yamane, Mukta Vazir, and Darrin Beaupre; Frenel DeMorin, Nick Paras, Qi Huang, and Elizabeth Doherty for the compound synthesis; Andrew Tasker and Matthew Lee for the helpful discussions; Kathryn Boorer (Amgen, Inc.) for the editorial assistance; and Glenn Begley for his support and critical reading of the manuscript.

The costs of publication of this article were defrayed in part by the payment of page charges. This article must therefore be hereby marked *advertisement* in accordance with 18 U.S.C. Section 1734 solely to indicate this fact.

Received 02/23/2010; revised 05/18/2010; accepted 05/28/2010; published OnlineFirst 07/27/2010.

References

1. Leicht DT, Balan V, Kaplun A, et al. Raf kinases: function, regulation and role in human cancer. Biochim Biophys Acta 2007;1773:1196–212.
2. Shaul YD, Seger R. The MEK/ERK cascade: from signaling specificity to diverse functions. Biochim Biophys Acta 2007;1773:1213–26.
3. Wojnowski L, Zimmer AM, Beck TW, et al. Endothelial apoptosis in Braf-deficient mice. Nat Genet 1997;16:293–7.
4. Wojnowski L, Stancato LF, Zimmer AM, et al. Craf-1 protein kinase is essential for mouse development. Mech Dev 1998;76:141–9.
5. Wojnowski L, Stancato LF, Larner AC, Rapp UR, Zimmer A. Overlapping and specific functions of Braf and Craf-1 proto-oncogenes during mouse embryogenesis. Mech Dev 2000;91:97–104.
6. Marais R, Light Y, Paterson HF, Mason CS, Marshall CJ. Differential regulation of Raf-1, A-Raf, and B-Raf by oncogenic ras and tyrosine kinases. J Biol Chem 1997;272:4378–83.
7. Wiese S, Pei G, Karch C, et al. Specific function of B-Raf in mediating survival of embryonic motoneurons and sensory neurons. Nat Neurosci 2001;4:137–42.
8. Mercer K, Chiloeches A, Huser M, Kiernan M, Marais R, Pritchard C. ERK signalling and oncogene transformation are not impaired in cells lacking A-Raf. Oncogene 2002;21:347–55.
9. Pritchard CA, Bolin L, Slattery R, Murray R, McMahon M. Post-natal lethality and neurological and gastrointestinal defects in mice with targeted disruption of the A-Raf protein kinase gene. Curr Biol 1996;6:614–7.
10. Pritchard CA, Samuels ML, Bosch E, McMahon M. Conditionally oncogenic forms of the A-Raf and B-Raf protein kinases display different biological and biochemical properties in NIH 3T3 cells. Mol Cell Biol 1995;15:6430–42.
11. Bosch E, Cherwinski H, Peterson D, McMahon M. Mutations of critical amino acids affect the biological and biochemical properties of oncogenic A-Raf and Raf-1. Oncogene 1997;15:1021–33.
12. Sharma PS, Sharma R, Tyagi T. Receptor tyrosine kinase inhibitors as potent weapons in war against cancers. Curr Pharm Des 2009;15:758–76.
13. Thompson N, Lyons J. Recent progress in targeting the Raf/MEK/ERK pathway with inhibitors in cancer drug discovery. Curr Opin Pharmacol 2005;5:350–6.
14. Roberts PJ, Der CJ. Targeting the Raf-MEK-ERK mitogen-activated protein kinase cascade for the treatment of cancer. Oncogene 2007;26:3291–310.
15. Davies H, Bignell GR, Cox C, et al. Mutations of the BRAF gene in human cancer. Nature 2002;417:949–54.
16. Wellbrock C, Karasarides M, Marais R. The RAF proteins take centre stage. Nat Rev Mol Cell Biol 2004;5:875–85.
17. Lyons JF, Wilhelm S, Hibner B, Bollag G. Discovery of a novel Raf kinase inhibitor. Endocr Relat Cancer 2001;8:219–25.
18. King AJ, Patrick DR, Batorsky RS, et al. Demonstration of a genetic therapeutic index for tumors expressing oncogenic BRAF by the kinase inhibitor SB-590885. Cancer Res 2006;66:11100–5.
19. Ramurthy S, Subramanian S, Aikawa M, et al. Design and synthesis of orally bioavailable benzimidazoles as Raf kinase Inhibitors. J Med Chem 2008;51:7049–52.
20. Tsai J. Discovery of a selective inhibitor of oncogenic B-Raf kinase with potent antimelanoma activity. Proc Natl Acad Sci U S A 2008;105:3041–6.
21. Hoeflich KP, Herter S, Tien J, et al. Antitumor efficacy of the novel RAF inhibitor GDC-0879 is predicted by BRAFV600E mutational status and sustained extracellular signal-regulated kinase/mitogen-activated protein kinase pathway suppression. Cancer Res 2009;69:3042–51.
22. Solit DB, Garraway LA, Pratilas CA, et al. BRAF mutation predicts sensitivity to MEK inhibition. Nature 2006;439:358–62.
23. Flaherty K, Puzanov I, Sosman J, et al. Phase I study of PLX4032: proof of concept for V600E BRAF mutation as a therapeutic target in human cancer. J Clin Oncol 2009;27:15S; abstr 9000.
24. Puzanov I, Nathanson KL, Chapman PB, et al. PLX4032, a highly selective V600EBRAF kinase inhibitor: clinical correlation of activity with pharmacokinetic and pharmacodynamic parameters in a phase I trial. J Clin Oncol 2009;27:15s; abstr 9021.
25. Smith AL, DeMorin FF, Paras NA, et al. Selective inhibitors of the mutant B-Raf pathway: discovery of a potent and orally bioavailable aminoisoquinoline. J Med Chem 2009;52:6189–92.
26. Van Gompel JJ, Kunnimalaiyaan M, Holen K, Chen H. ZM336372, a Raf-1 activator, suppresses growth and neuroendocrine hormone levels in carcinoid tumor cells. Mol Cancer Ther 2005;4:910–7.
27. Kappes A, Vaccaro A, Kunnimalaiyaan M, Chen H. ZM336372, a Raf-1 activator, inhibits growth of pheochromocytoma cells. J Surg Res 2006;133:42–5.

Published OnlineFirst July 27, 2010; DOI: 10.1158/1535-7163.MCT-10-0181

28. Houben R, Ortmann S, Schrama D, et al. Activation of the MAP kinase pathway induces apoptosis in the Merkel cell carcinoma cell line UISO. J Invest Dermatol 2007;127:2116–22.
29. Mueller BM, Romerdahl CA, Trent JM, Reisfeld RA. Suppression of spontaneous melanoma metastasis in scid mice with an antibody to the epidermal growth factor receptor. Cancer Res 1991;51:2193–8.
30. Brattain MG, Fine WD, Khaled FM, Thompson J, Brattain DE. Heterogeneity of malignant cells from a human colonic carcinoma. Cancer Res 1981;41:1751–6.
31. Giard DJ, Aaronson SA, Todaro GJ, et al. *In vitro* cultivation of human tumors: establishment of cell lines derived from a series of solid tumors. J Natl Cancer Inst 1973;51:1417–23.
32. Sharma SV, Bell DW, Settleman J, Haber DA. Epidermal growth factor receptor mutations in lung cancer. Nat Rev Cancer 2007;7:169–81.
33. Duncia JV, Santella JB III, Higley CA, et al. MEK inhibitors: the chemistry and biological activity of U0126, its analogs, and cyclization products. Bioorg Med Chem Lett 1998;8:2839–44.
34. Hall-Jackson CA, Eyers PA, Cohen P, et al. Paradoxical activation of Raf by a novel Raf inhibitor. Chem Biol 1999;6:559–68.
35. Santos SDM, Verveer PJ, Bastiaens PIH. Growth factor-induced MAPK network topology shapes Erk response determining PC-12 cell fate. Nat Cell Biol 2007;9:324–30.
36. Yen I, Song K, Stokoe S, et al. Understanding the effects of RAF inhibitors on RAF signaling in B-RAF V600E mutant versus wild type tumors. Mol Cancer Ther 2009:B90.
37. Heidorn SJ, Milagre C, Whittaker S, et al. Kinase-dead BRAF and oncogenic RAS cooperate to drive tumor progression through CRAF. Cell 2010;140:209–21.
38. Hatzivassiliou G, Song K, Yen Y, et al. RAF inhibitors prime wild-type RAF to activate the MAPK pathway and enhance growth. Nature 2010, doi: 10.1038/nature08833.
39. Carnahan J, Beltran P, Babij C, et al. Selective and potent inhibitors of the mutant B-Raf pathway paradoxically stimulate the MAPK pathway in wild-type B-Raf cells. Proceedings of the 101st Annual Meeting of the American Association for Cancer Research. Washington (DC):2010, p. Abstr #21.
40. Robert C, Mateus C, Spatz A, Wechsler J, Escudier B. Dermatologic symptoms associated with the multikinase inhibitor sorafenib. J Am Acad Dermatol 2009;60:299–305.
41. Beldner M, Jacobson M, Burges GE, Dewaay D, Maize JC, Jr., Chaudhary UB. Localized palmar-plantar epidermal hyperplasia: a previously undefined dermatologic toxicity to sorafenib. Oncologist 2007;12:1178–82.
42. Hong DS, Reddy SB, Prieto VG, et al. Multiple squamous cell carcinomas of the skin after therapy with sorafenib combined with tipifarnib. Arch Dermatol 2008;144:779–82.
43. Poulikakos P, Joseph E, Tsai J, Bollag G, Rosen N. The RAF inhibitor PLX4032 effectively suppresses MAPK signaling in cells harboring mutant BRAF, but not in cells with upstream activation of the pathway. AACR Meeting Abstracts 2008 April 12, 2008;2008:5800.

AACR American Association for Cancer Research

Molecular Cancer Therapeutics

Selective and Potent Raf Inhibitors Paradoxically Stimulate Normal Cell Proliferation and Tumor Growth

Josette Carnahan, Pedro J. Beltran, Carol Babij, et al.

Mol Cancer Ther 2010;9:2399-2410. Published OnlineFirst July 27, 2010.